

## Modeling of 18-Pulse STATCOM for Power System Applications

Bhim Singh\* and R. Saha†

†\*Department of Electrical Engineering, Indian Institute of Technology, Delhi, New Delhi, India

### ABSTRACT

A multi-pulse GTO based voltage source converter (VSC) topology together with a fundamental frequency switching mode of gate control is a mature technology being widely used in static synchronous compensators (STATCOMs). The present practice in utility/industry is to employ a high number of pulses in the STATCOM, preferably a 48-pulse along with matching components of magnetics for dynamic reactive power compensation, voltage regulation, etc. in electrical networks. With an increase in the pulse order, need of power electronic devices and inter-facing magnetic apparatus increases multi-fold to achieve a desired operating performance. In this paper, a competitive topology with a fewer number of devices and reduced magnetics is evolved to develop an 18-pulse, 2-level  $\pm 100$ MVAR STATCOM in which a GTO-VSC device is operated at fundamental frequency switching gate control. The inter-facing magnetics topology is conceptualized in two stages and with this harmonics distortion in the network is minimized to permissible IEEE-519 standard limits. This compensator is modeled, designed and simulated by a SimPowerSystems tool box in MATLAB platform and is tested for voltage regulation and power factor correction in power systems. The operating characteristics corresponding to steady state and dynamic operating conditions show an acceptable performance.

**Keywords:** Fast Fourier transformation, gate-turn off thyristor, magnetics, STATCOM, total harmonic distortion, voltage source converter

### 1. Introduction

For high power rating compensators, a GTO-VSC (gate-turn off thyristor based voltage source converter) based STATCOM [1-8], in which self commutating solid state device GTOs are gated once per cycle of power frequency, is widely used and mature technology for dynamic reactive power compensation through generation and absorption of controllable reactive power.

An elementary six-pulse GTO-VSC connected with a DC capacitor produces a square wave or a quasi-square wave voltage output in fundamental frequency gate switching. This waveform would contain harmonics of the order of  $6N \pm 1$ , where  $N= 1, 2, 3 \dots$  etc. In multi-pulse configuration, a number ( $P$ ) of elementary six-pulse VSC waveforms are electro-magnetically added to produce a multi-pulse ( $6P$  pulses,  $P=1, 2, 3, 4 \dots$  number of six pulse VSC) waveform which contains harmonics in the order of  $6NP \pm 1$ . For example, a 48-pulse VSCs constituted with 8x6-pulse elementary VSCs will have 47<sup>th</sup>, 49<sup>th</sup>, 95<sup>th</sup>, 97<sup>th</sup> harmonics in its output AC voltage waveform. Obviously, in multi-pulse topology, the harmonics are greatly attenuated with an increase in the number of 6-pulse VSCs; an output voltage close to sinusoidal waveform is

Manuscript received April 19, 2006; revised March. 6, 2007

† Corresponding Author: rshahacno@yahoo.com

Tel: +91-011-26591045, Central Electricity Authority, Sewa Bhawan, R. K. Puram, New Delhi, India.

\*Department of Electrical Engineering, Indian Institute of Technology, Delhi, New Delhi, India.

realized. Thus, the need for power electronic devices increases linearly with the higher pulse order STATCOM and the requirement of magnetics would also realize a manifold increase. A 3x6 multi-pulse VSC configuration having gate triggering at a displacement angle of  $20^\circ$  generally achieves an 18-pulse voltage waveform after adding electro-magnetically the three AC output voltages of the VSCs through coupling transformer(s). The summed-up voltage would contain harmonics of the order of  $18N \pm 1$  ( $N=1,2,\dots$ ) i.e.  $17^{\text{th}}$ ,  $19^{\text{th}}$ ,  $35^{\text{th}}$ ,  $37^{\text{th}}$ ...harmonics. In this paper, a new 18-pulse 2-level,  $\pm 100\text{MVAR}$  STATCOM model employing 3x6-pulse GTO-VSCs triggered once per cycle of fundamental frequency at a displacement angle of  $(+)20^\circ, 0^\circ$  and  $(-)20^\circ$ , inter-facing magnetics in two stages, with standard PI-control methodology

(stage-I) and this in turn, sets an electromagnetic coupling with AC system at PCC. In the control algorithm, PI controllers having a combination of outer voltage control loop and inner current control loop are configured to control reactive power by means of phase angle ( $\alpha$ ) control between the AC supply voltage and VSC output voltage. The compensator is modeled using a SimPowerSystems tool box in MATLAB platform and employed for voltage regulation as well as for load power factor correction to unity in var control mode. Results of simulation studies are illustrated and it was observed that the operating characteristics of the model were satisfying while the harmonic interference was considerably low for fitness of the compensator in the power system.

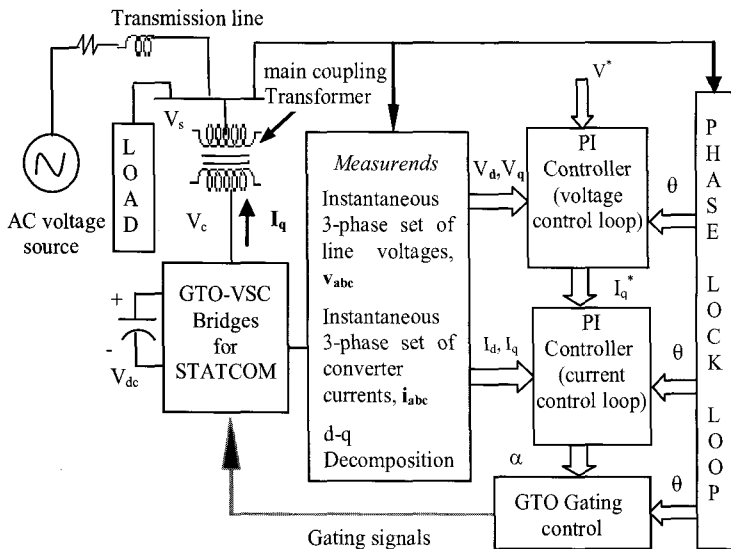


Fig. 1a GTO-VSC based STATCOM architecture and working principle

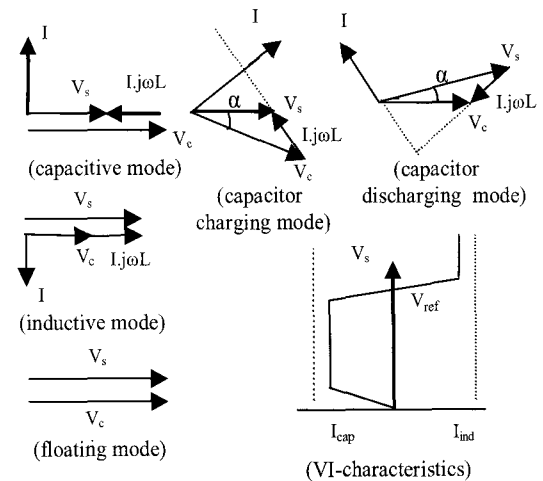


Fig. 1b STATCOM operating characteristics

and DC capacitor as an energy storage device, is designed and simulated in MATLAB platform. Inter-facing magnetics is designed rather in a different way to achieve an 18-pulse compensator of competitive performance in multi-pulse topology. Corresponding to each converter, a 3- $\phi$  inter-phase transformer is used in the first stage to step-up the VSC output voltage into the level of AC supply voltage. A newly designed phase shifting equipment providing a phase shift of  $20^\circ, 0^\circ, (-) 20^\circ$  to the three sets of decoupled voltage waveforms available from inter-phase transformers, were employed in stage-II of magnetics and cascaded with the inter-phase transformers

## 2. Working Principle of STATCOM

Figs. 1a-1b show the basic GTO-VSC based STATCOM architecture and operating principle. The main objective of STATCOM is to control reactive current flow by generation and absorption of controllable reactive power with various solid-state switching techniques. The essential components in a GTO-VSC based STATCOM are GTO-VSC bridge(s), DC capacitor (C) working as an energy storage device, inter-phase or inter-stage magnetics forming the electrical coupling between VSC bridges and

AC system, and a controller generating gating signal.

A controllable three-phase AC output voltage waveform close to sinusoidal nature is obtained at the point of common coupling (PCC). The output AC voltage of the VSC ( $V_c$ ) is governed by a DC capacitor voltage ( $V_{dc}$ ), which can be controlled by varying phase difference ( $\alpha$ ) between  $V_c$  and  $V_s$  (supply voltage). An almost sinusoidal current in quadrature with the line voltage is injected into the electrical system emulating an inductive or a capacitive reactance at PCC. The magnitude of the quadrature component of the VSC current ( $I_q$ ) regulates the phase difference ( $\alpha$ ) between  $V_c$  and  $V_s$  across the transformer leakage reactance ( $X$ ), which in turn controls reactive power flow. Fig. 1b shows the basic operating principle of a GTO-VSC based STATCOM. When  $V_c > V_s$ , the STATCOM is considered to be operating in a capacitive mode and when  $V_c < V_s$ , it is operating in an inductive mode and for  $V_c = V_s$ , no reactive power exchange takes place and STATCOM is said to be operating in floating mode. However, a small phase difference ( $\alpha$ ) is maintained so that VSC losses are compensated by active power drawn from AC system. Employing phase angle control ( $\alpha$ ) between  $V_c$  and  $V_s$ ,  $V_{dc}$  is controlled with charging or discharging of the capacitor and thus capacitive or inductive or floating mode of operation is emulated to control reactive power flow in the AC system.

### 3. Model of STATCOM

Fig. 2 and Fig. 3 show the schematic layout and the detailed circuit configuration of the  $\pm 100$ MVAR, 18-pulse STATCOM model respectively. It is achieved by 3x6-pulse GTO-VSCs operated at displacement angle of  $20^\circ$ ,  $0^\circ$  and  $-20^\circ$  in fundamental frequency switching gate control. The VSCs are connected in parallel on the DC side with an energy storing DC capacitor (15000 $\mu$ F) and decoupled AC sides are connected to secondary sides (5.1kV) of the three 3- $\phi$ , 35MVA, 5.1/132kV transformers (stage-I), termed hereafter inter-phase transformers. A newly designed phase shifting device (stage-II), termed hereafter phase shifter, is cascaded with the inter-phase transformers and setting an electromagnetic coupling with AC system at PCC. This provides a phase shift of  $20^\circ$ ,  $0^\circ$ ,

$(-20^\circ)$  to the three sets of decoupled voltage waveforms available from inter-phase transformers. The AC system is represented by Thevenin equivalent voltage source with a short circuit level of about 3000MVA and X/R ratio equal to 10. PI-controllers are employed which consist of inner current control loop that controls  $\alpha$ , and outer voltage control loop that determines the reference reactive current ( $I_q^*$ ) for the inner loop.

### 3.1 Magnetics

As mentioned above, the inter-facing magnetics for the 18-pulse compensator model has been conceptualized in two stages viz. stage-I and stage-II. In stage-I, three numbers 3- $\phi$  inter-phase transformers each with a rating of 35MVA,  $\Delta$ - $\Delta$ , 5.1/132kV, are employed (Fig. 2 and Fig. 3) to step-up VSC output AC voltage to 132kV level. Each of these 3- $\phi$  transformers is modeled employing three sets of identical 2-winding linear type single-phase transformer units. In stage-II, the phase shifter is designed to provide phase shifts of  $20^\circ$ ,  $0^\circ$ ,  $(-20^\circ)$  to the three sets of decoupled voltages (132kV) of inter-phase transformers, which in turn sets an electromagnetic coupling with AC system at PCC. This is modeled with six number 3-winding single-phase transformer units having winding connections as illustrated in Fig. 4a. It has basically three legs - leg-1, leg-2 and leg-3. A leg comprises of a set of two number 3-winding linear transformers, each having a main (M), long (L) and short (S) windings. In leg-1, the main two windings are connected in parallel and the two short windings with one of its terminals free, are connected to the main windings. The turn ratios between main and short windings are so determined that the voltage level across the free terminals of the short windings is equal to the magnitude of the line voltage. The two L-windings with one of its terminals free (i.e. B" and B') are connected to the main winding of leg-2 and leg-3. The turn ratio of main and long windings are so designed that it would enable to provide a phase shift of  $\pm 20^\circ$  to the voltages at terminals B" and B'. In leg-2, M-windings and S-windings are similarly connected. The L-windings with one of its terminal free (i.e. R" and R') are connected to the main windings of leg-1 and leg-3. In leg-3, M-windings and S-windings are also similarly connected. The L-windings with one of its terminal free

(i.e.  $Y''$  and  $Y'$ ) are connected to the main windings of leg-1 and leg-2. The free terminals of L-windings of leg-1, leg-2 and leg-3 i.e.  $B''$ ,  $B'$ ,  $R''$ ,  $R'$ ,  $Y''$  and  $Y'$ , constitute three symmetrical sets of three phase, 132kV balanced phasors R-Y-B, R'-Y'-B' and R''-Y''-B'', each having a  $\Delta$ - $\Delta$  vector configuration with a phase displacement of  $0^\circ$ ,  $20^\circ$ (lead), and  $-20^\circ$ (lag) respectively. The phasor diagram of the three sets of 132kV phasors R'-Y'-B', R-Y-B and R''-Y''-B'', is shown in Fig. 4b. Design parameters of inter-phase transformers and phase shifter are provided in

the Appendix.

### 4. MATLAB Model and Operation of STATCOM

Fig. 5a exhibits the MATLAB model diagram of the proposed STATCOM and Figs. 5b-5c illustrate detailed models of the interfacing magnetics i.e. stage-I and stage-II respectively.

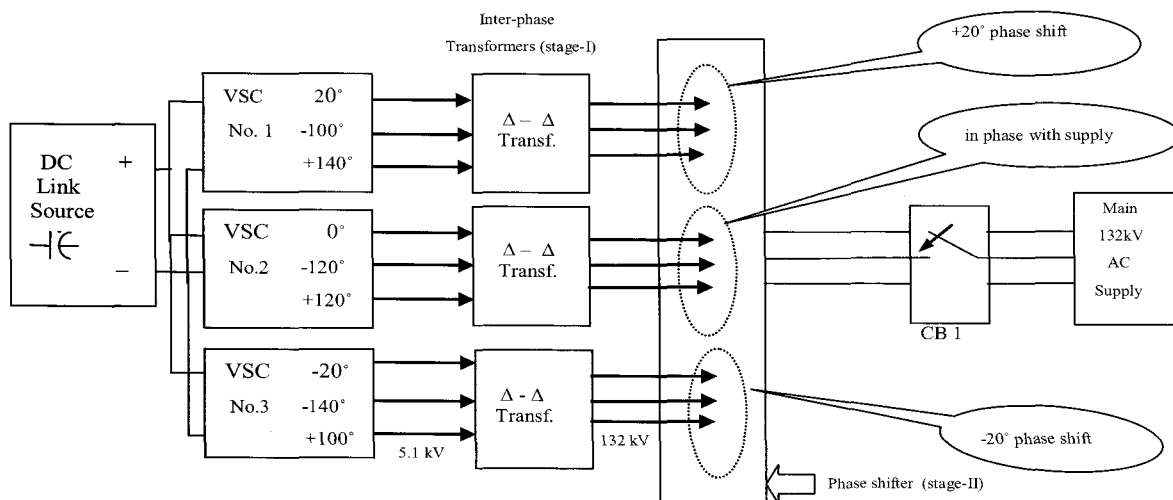


Fig. 2 Schematic layout of 3x6-pulse STATCOM network configuration

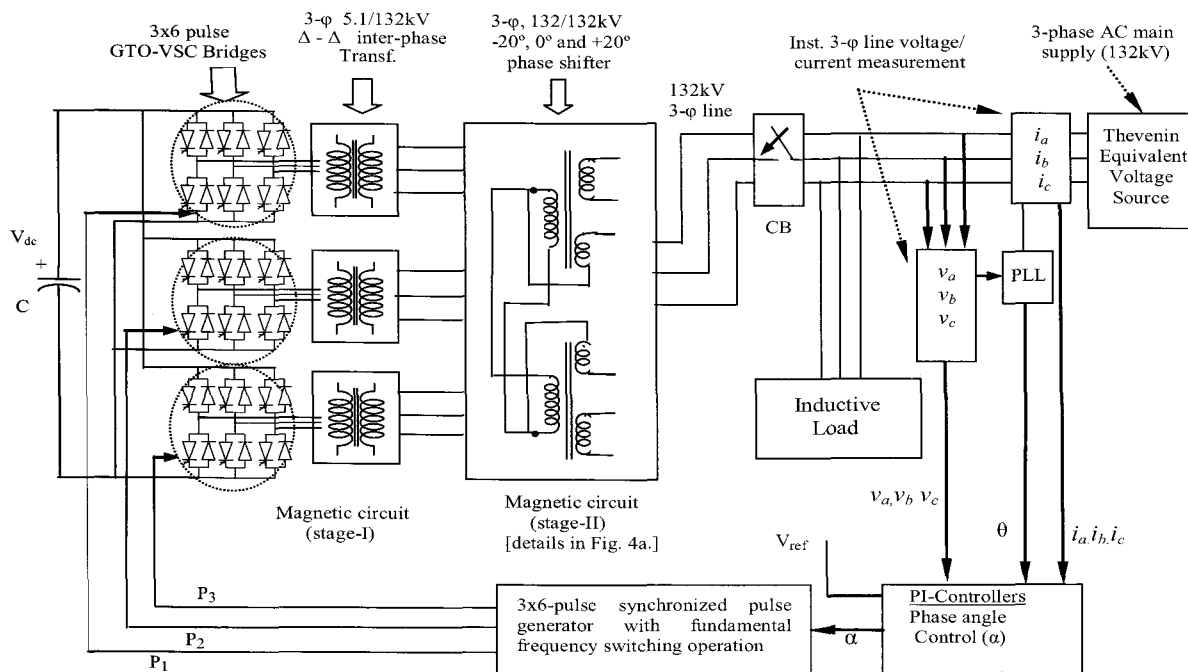


Fig. 3 System configuration of  $\pm 100$ MVAR 3x6 pulse STATCOM

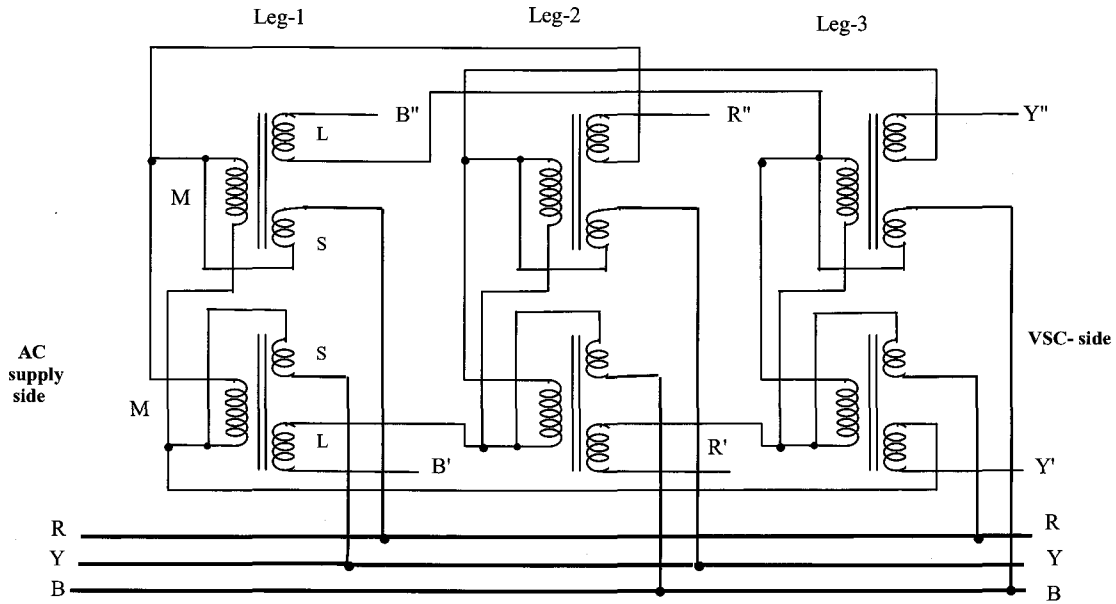


Fig. 4a (+) 20°-0°-(-)20° phase shifter employing 3-winding Transformers

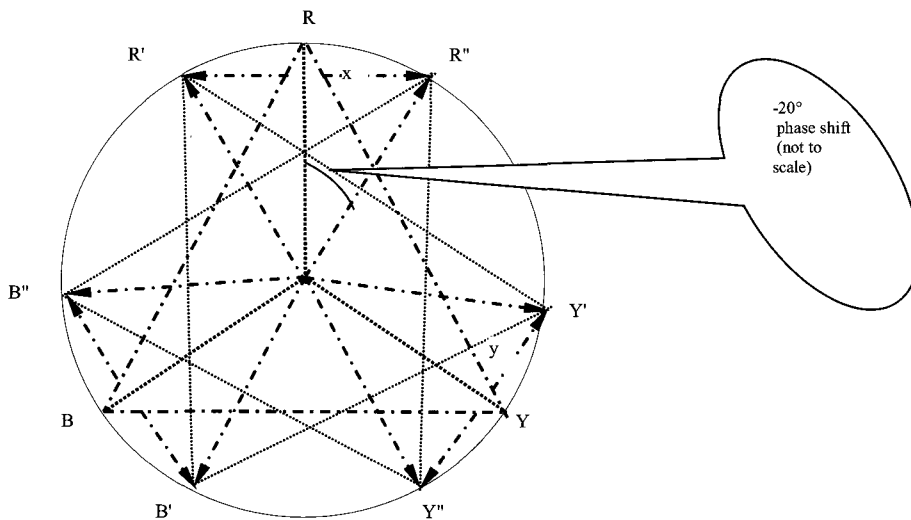


Fig. 4b +20°-0°-(-)20° phase shifter phasor diagram

The main AC system is represented by the Thevenin equivalent voltage source, which supplies the reactive load in the network radially. As shown in the STATCOM model (Fig. 1a and Fig. 5a), the AC voltages and currents (instantaneous values) are sensed in time domain using proper sensors and synthesized/decomposed by d-q synchronous rotating axis transformation. Phase Lock Loop (PLL) is employed to calculate phase and frequency information of the fundamental positive sequence

component of system voltage, which synchronizes converter AC output voltage. After decomposition of instantaneous AC supply voltages ( $v_a, v_b, v_c$ ) and currents ( $i_a, i_b, i_c$ ) into d-q frame, the transformed value of voltage,  $V_{dq}(=\sqrt{V_d^2+V_q^2})$  and current,  $I_q$  are processed by the PI controller to derive the compensating signal for synchronized 18-pulse generator which initiates the gating of the converters. In this process, the outer control loop (Fig. 6a) produces the desired reference reactive current

$I_q^*$  based on the voltage error signal ( $V^* - V_{dq}$ ). While on the other hand, the inner current loop (Fig. 6b) produces the phase angle ( $\alpha$ ) control signal for generating the required gating pulses for the converters. An almost sinusoidal current in quadrature with the line voltage emulating an inductive or a capacitive reactance is injected at PCC. The parameters of various components of

the model are given in the Appendix. With the reference voltage ( $V^*$ ) set at desired values (viz. 1.0pu, 1.03pu and 0.97pu) and considering high inductive loads (0.85pf) being supplied from AC mains, the operating performance of the STATCOM in the network was studied under various operating conditions.

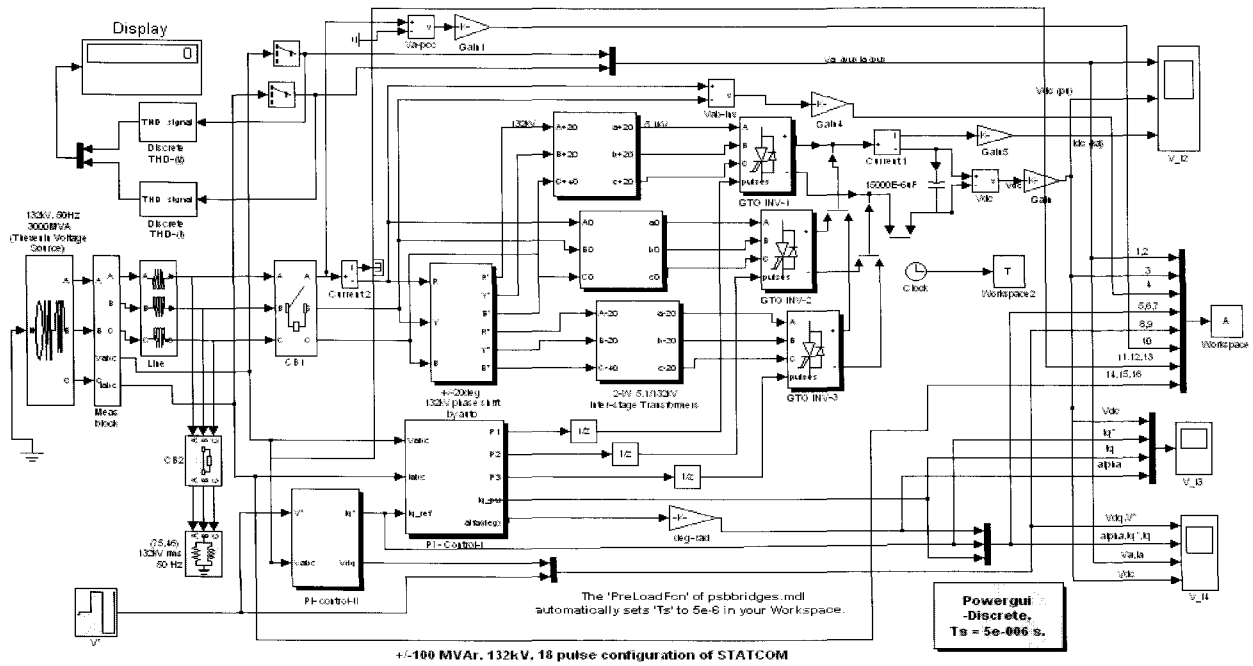


Fig. 5a MATLAB model of  $\pm 100$ MVAR 18-pulse STATCOM

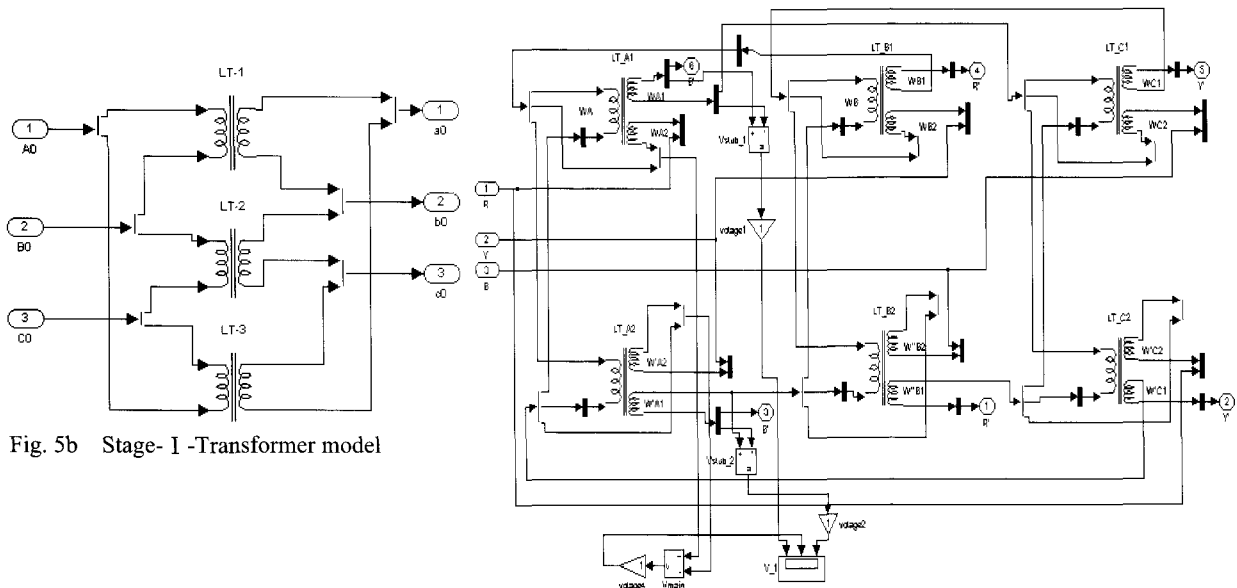


Fig. 5b Stage-I -Transformer model

Fig. 5c Stage-II - Transformer connections of phase shifter model for  $20^\circ$  (lead),  $0^\circ$ , and  $-20^\circ$  (lag) phase shifts

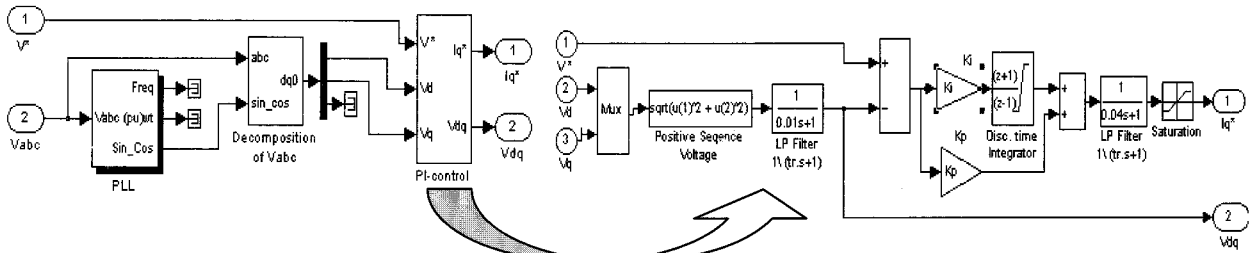


Fig. 6a Outer voltage control loop circuit

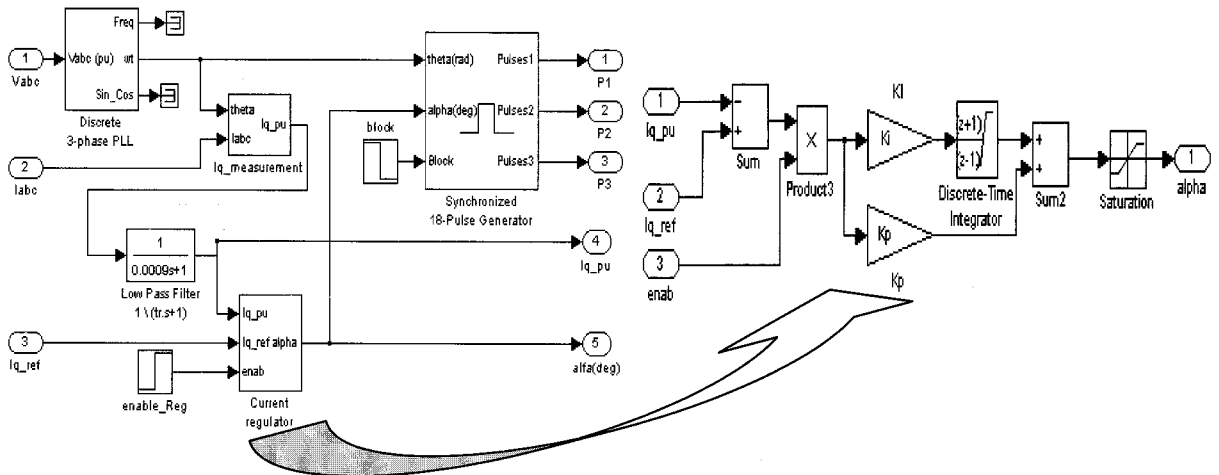


Fig. 6b Inner current control loop circuit

5. Results and Discussion

The proposed 18-pulse STATCOM model was simulated as a dynamic reactive power compensator in MATLAB platform for voltage regulation and power factor correction in electrical networks. The staircase line-to-line voltage waveform generated at PCC across the terminals (open) of the proposed 18-pulse compensator is shown in Fig. 7.

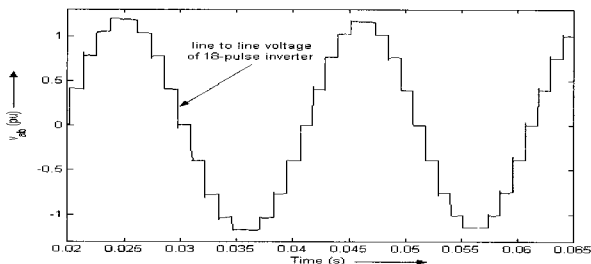


Fig. 7 18-pulse STATCOM AC terminal (open) voltage at PCC

5.1 Steady State Operation

The operating performance characteristics of the model are analyzed during steady state and dynamic operating conditions corresponding to the load of 75MW/65MW/55MW with its power factor of 0.85 (lag). The FFT tool available in MATLAB is used to obtain load voltage and current harmonic spectra for various operating conditions and to determine respective THD values.

5.1.1 Voltage Regulation

Presuming that STATCOM would be operated as a voltage regulator, the reference line voltage  $V^*$  is set to 1.0pu, 1.03pu and 0.97pu during the intervals (0s-0.22s), (0.22s-0.42s) and (0.42s-0.62s) respectively. The reference value of the capacitive reactive current limit is set to  $I_q^* = 1.2pu$  and inductive reactive current limit at  $I_q^* = -1.2pu$  in the voltage control loop. With the DC capacitor (C) pre-charged and total simulation time set to 0.62s with a sampling time of  $5e^{-6}s$ , the time-domain operating

characteristics of system parameters ( $v_a, v_b, v_c$ ), ( $i_a, i_b, i_c$ ), ( $v_{a-pcc}, v_a$ ), ( $v_a, i_a$ ), ( $V^*, V_{dq}$ ),  $V_{dc}$ , ( $\alpha, I_q^*, I_q$ ) corresponding to an inductive load of (75MW, 0.85pf) and related harmonic spectrum analysis during steady state conditions are exhibited in Figs. 8a-8f. The sinusoidal phase load voltage ( $v_a, v_b, v_c$ ) and current ( $i_a, i_b, i_c$ ) waveforms during the total simulation period are illustrated in Fig. 8a. It is seen from the operating characteristics (Fig. 8b) that prior to STATCOM being put into operation, both the active and reactive power requirements of the load of 75MW, 0.85pf (lag) are met from the supply and the supply current  $i_a$  (phase-a) lags the line voltage  $v_a$  (phase-a). When CB1, as shown in Fig. 5a, is switched on at the instant of 0.04s and the proposed STATCOM is put into operation, it is seen from the ( $V^*, V_{dq}$ ) characteristics (Fig. 8b) that the line voltage (decomposition value of the measured load voltages,  $V_{dq}$ ) is closely following  $V^*=1.0pu$  during the interval (0.04s-0.22s). Again, during the interval (0.22s-0.42s) when  $V^*$  is set to 1.03pu, it is seen from the ( $v_a, i_a$ ) and ( $V^*, V_{dq}$ ) characteristics (Fig. 8b) that the supply current  $i_a$  leads  $v_a$  and the voltage control loop is producing the desired reference reactive current ( $I_q^*$ ) for the current loop and maintains a constant load voltage at its reference value ( $V^*=1.03pu$ ) emulating the compensator as a capacitive reactance.

Similarly, during the interval (0.42s-0.62s) when  $V^*$  is set to 0.97pu, it is seen from the ( $v_a, i_a$ ) and ( $V^*, V_{dq}$ ) characteristics (Fig. 8b) that the supply current  $i_a$  lags  $v_a$  with the controller regulating the reference inductive reactive current ( $I_q^*$ ) within limits to maintain the constant load voltage at its reference value ( $V^*=0.97pu$ ) emulating the compensator as an inductive reactance. It has been also established from the performance characteristics that phase angle ( $\alpha$ ) control enables it to regulate  $V_{dc}$  across the DC capacitor, which in turn provides smooth and rapid control of load voltage at reference values within a couple of cycles in the intervals (0.1s-0.22s), (0.22-0.42s) and (0.42-0.62s).

For testing the behavior of the model in case of different inductive loads in the network viz. (65MW, 0.85pf) and (55MW, 0.85pf), the compensator is also found to have exhibited the similar operating performance characteristics. The voltage and current THD values

derived by FFT tools are shown in Table-1 for relative assessment of the results.

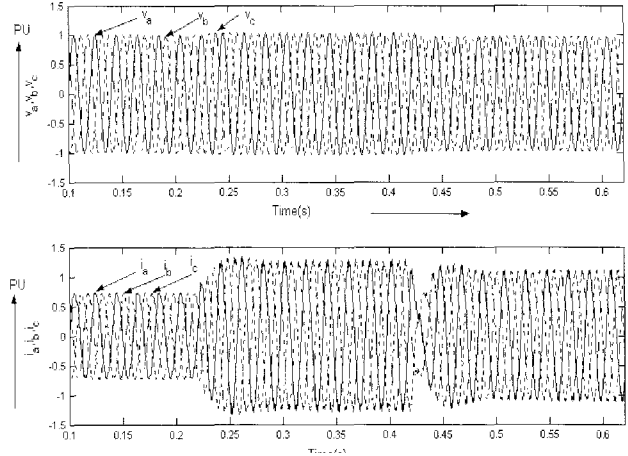


Fig. 8a Three phase instantaneous voltage( $v_a, v_b, v_c$ ) and current ( $i_a, i_b, i_c$ ) with 75MW 0.85pf lagging load when  $V^*$  sets at 1.0pu, 1.03pu and 0.97pu

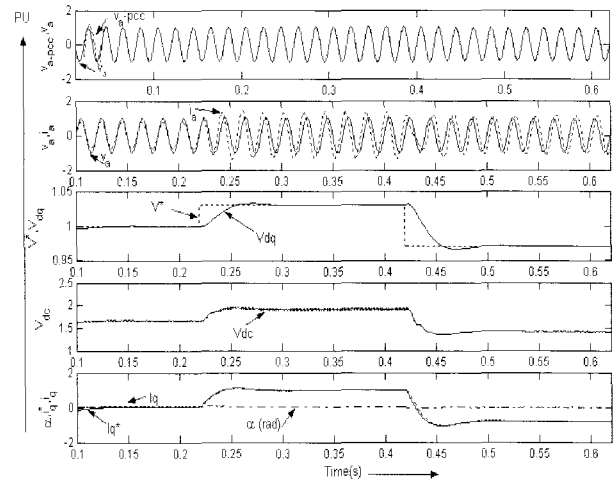


Fig. 8b Operating characteristics in voltage regulation mode for 70MW, 0.85pf(lag) load

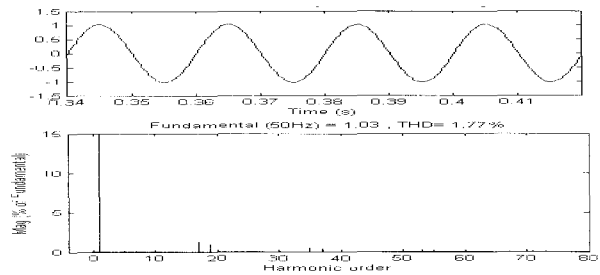


Fig. 8c Voltage( $v_a$ ) spectrum in capacitive mode



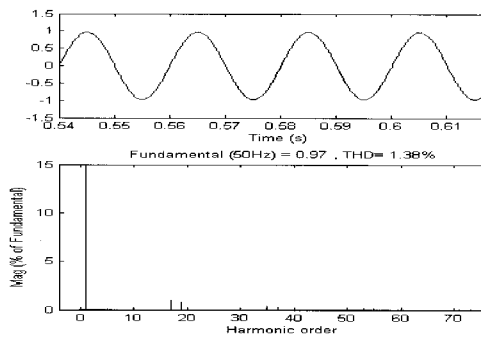


Fig. 8d Voltage spectrum ( $v_a$ ) in inductive mode

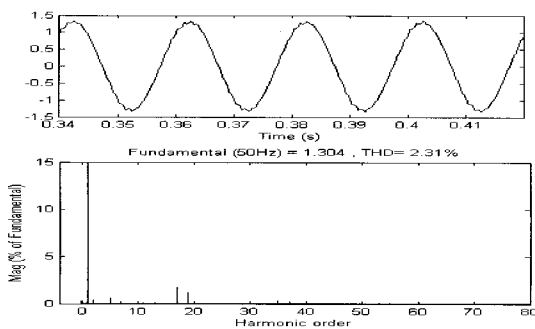


Fig. 8e Current ( $i_a$ ) spectrum in capacitive mode

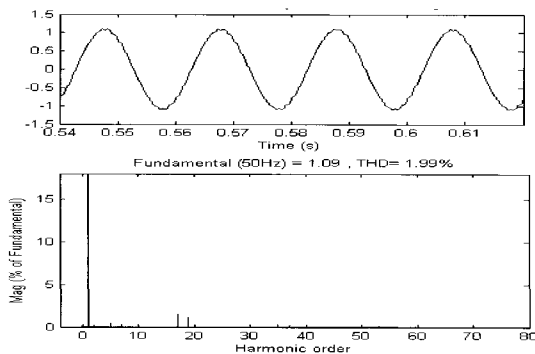


Fig. 8f Current spectrum ( $i_a$ ) in inductive mode

### 5.2 Load Power Factor Correction to Unity (upf) in var Control Mode

With outer voltage control loop made inactive in the compensator circuit (Fig. 5a), DC capacitor (C) pre-charged initially and with an inductive load of (75MW 0.85pf) in the network, simulation studies is performed by switching on the compensator (Fig. 5a) at the instant of 0.04s in a total simulation period of 0.30s. The time-domain operating performances characteristics of system parameters  $v_{a-pcc}$ , ( $v_a, i_a$ ), load pf angle( $\phi$ ),  $V_{dc}$

and ( $\alpha, I_q^*, I_q$ ) as observed from the simulation studies is illustrated in Fig. 9a. Figs. 9b- 9c illustrate the voltage and current harmonic spectra respectively.

It is seen from Fig. 9a that prior to STATCOM being put into operation (i.e. before 0.04s), both the active and reactive power requirements of the load are met from the supply and supply current  $i_a$  lags in the line voltage  $v_a$  at a pf angle of  $31.788^\circ$  (i.e.0.85pf). While the STATCOM is switched into operation at the instant of 0.04s (2-cycles), it is seen from ( $v_a, i_a$ ) waveforms (Fig. 9a) that  $v_a$  and  $i_a$  phasors are in the same phase (i.e. zero pf angle) enabling power factor correction form 0.85pf lag to unity. The supply current,  $i_a$  has the smaller value capable of supplying full power to the load as the compensator supplies the reactive power required by the load.

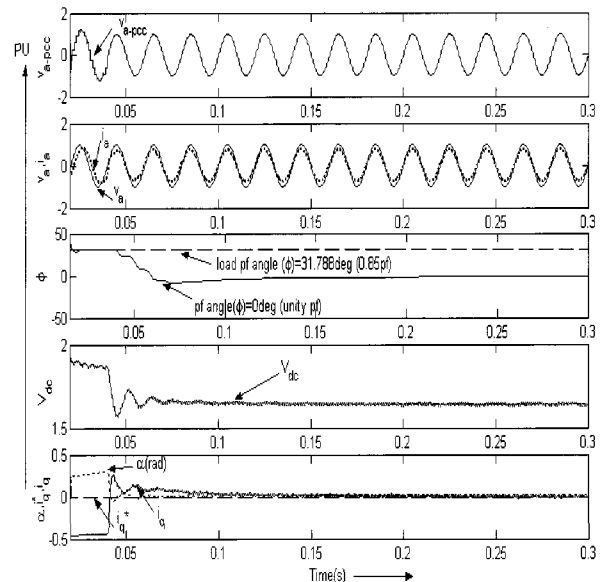


Fig. 9a Operating characteristics for unity power factor (upf) Correction in var control mode for 75MW, 0.85pf(lag) load

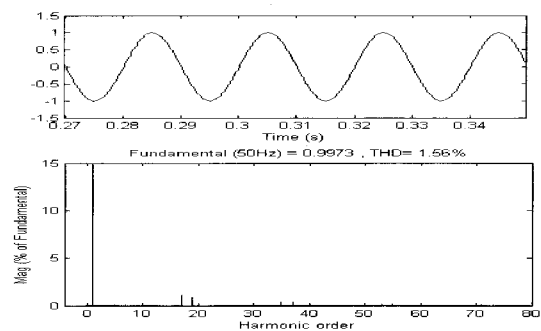


Fig. 9b Voltage harmonics( $v_a$ ) spectrum for upf correction

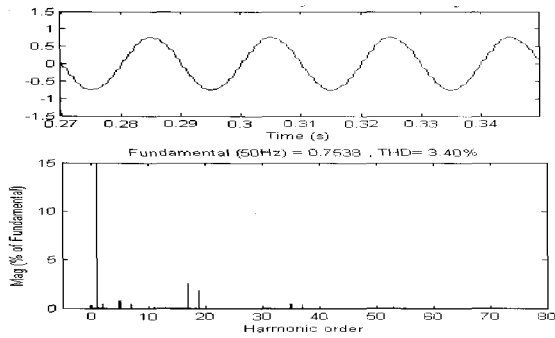


Fig. 9c Current harmonics( $i_a$ ) spectrum for upf correction

For testing the behavior of the model for different inductive loads in the network viz. (65MW, 0.85pf) and (55MW, 0.85pf), the simulation exercises for upf correction to the load show that the model performs well satisfying the system requirements. The voltage and current THD values derived by FFT tools during upf operation are shown in Table-2 for relative assessment of the results.

### 5.3 Dynamic Characteristics

While the compensator is employed for voltage regulation, it is seen from the performance characteristics (Fig. 8b) that while reference voltage  $V^*$  is dynamically changed from 1.0pu to 1.03pu and from 1.03pu to 0.97pu at the instant of 0.22s and 0.42s respectively, the compensator responds quickly as expected within a couple of cycles. The controller provides necessary damping to rapidly settle steady states for smooth operation of the system. No major overshoots or undershoots in voltage and current transients have been observed from the operating characteristics.

#### 5.3.1 Incremental Load Variation in Voltage Regulating Mode

With a reference voltage set to nominal value  $V^*=1.0$ pu in the outer control loop, DC capacitor (C) pre-charged initially in the compensator circuit (Fig. 5a) and the STATCOM is in service with an initial load of (70MW, 0.85pf lag) in the network, the behavior of the system parameters is studied with a total simulation period of 0.45s corresponding to load increased by 10% ( $\Delta$ -load=7MW, 0.85pf) dynamically at the instant of 0.24s. From the time-domain operating performance

characteristics as illustrated in Fig. 10a, it is seen that the incremental load change in the network does not impair stability of the system and the controller provides necessary damping for smooth functioning of the compensator. No major overshoot/undershoot in system voltage/current is experienced during the event. The harmonic distortion (Figs. 10b-10c and Table-3) following the insertion of the additional load is also observed to be minimal.

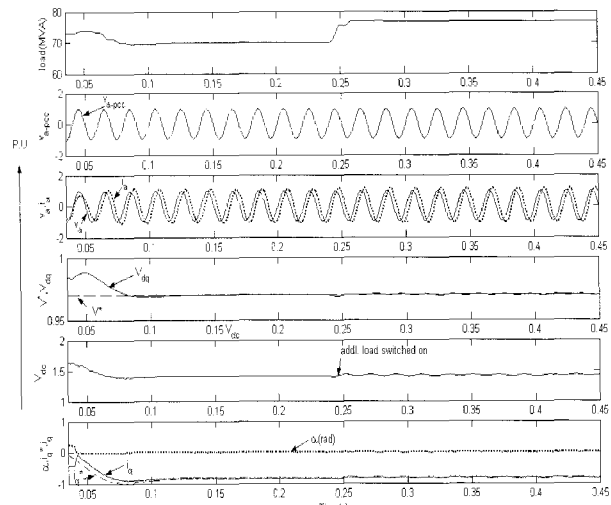


Fig. 10a Operating characteristics following 10% load injection at the instant of 0.24s in voltage regulation mode on 70MW, 0.85pf(lag) load

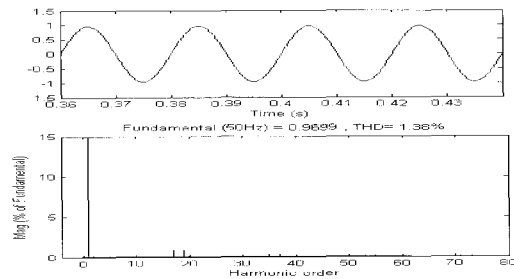


Fig. 10b Voltage harmonics ( $v_a$ ) spectrum after load variation

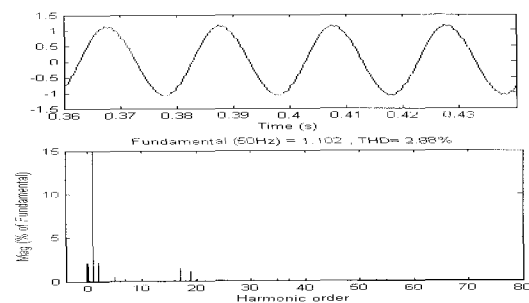


Fig. 10c Current harmonics ( $i_a$ ) spectrum after load variation

**5.3.2 Incremental Load Variation in var Control Mode**

With the outer voltage control loop made inactive in the compensator circuit (Fig. 5a), DC capacitor (C) pre-charged initially and the compensator is presumed to be in service with an inductive load of (70MW 0.85pf) in the network, behavior of the STATCOM is studied by dynamically increasing the load by 10% ( $\Delta$ -load=7MW, 0.85p) at the instant of 0.24s in a total simulation period of 0.40s. From the operating characteristics shown in Fig. 11a, it is observed that the system is operating at upf before and after the additional load being injected into the system. The system is well damped and there is no transient as such in voltage as well as current waveforms following the load insertion. Harmonic distortion (Figs. 11b-11c and Table-3) for such a change is also observed to be minimal.

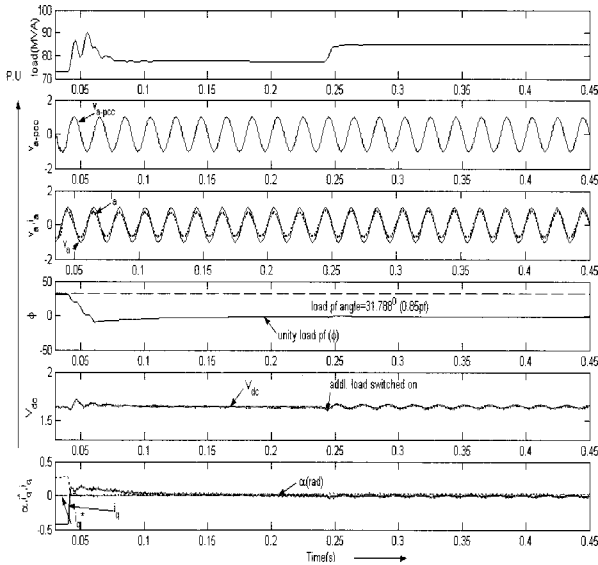


Fig. 11a Operating characteristics in var control mode for incremental Load variation of 10% at the instant of 0.24s on an initial load of 70MW, 0.85pf(lag)

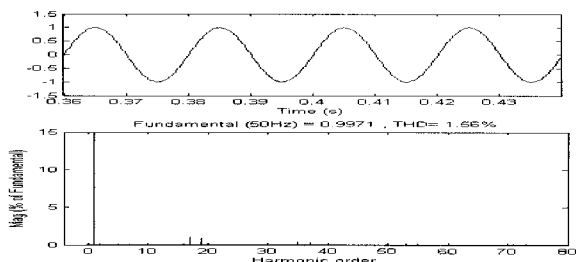


Fig. 11b Voltage harmonics ( $v_a$ ) spectrum after the load injection

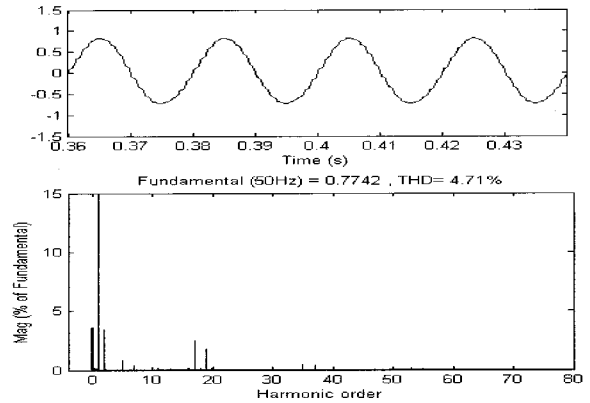


Fig. 11c Current harmonics ( $i_a$ ) spectrum after the load injection

**5.4 Voltage and Current Harmonics Interference**

While the STATCOM is in service and being operated either for voltage regulation or power factor correction, the voltage and current THDs are determined with the help of the FFT tool in MATLAB. Figs. 8c-8f exhibits the voltage and harmonic spectra corresponding to capacitive and inductive modes of operation of the compensator for an inductive load of (75MW, 0.85pf). In Table-1, voltage and current THD values derived from FFT analysis corresponding to the compensator being operated in regulating voltage are tabulated for inductive loads of (75MW 0.85pf), (65MW, 0.85pf) and (55MW, 0.85pf). It is seen that the THD levels are well within permissible limits.

While the compensator is operated in var control mode for upf correction, the voltage and current harmonic spectra which are derived by using the FFT tool corresponding to the inductive load of (75MW 0.85pf), is illustrated in Figs. 9b-9c. Table-2 provides the THD values derived by FFT analysis. It is seen that the THD levels are well within acceptable limits.

For the 10% incremental load change in the network at the instant of 0.24s against an initial load of (70MW,0.85pf lag) and compensator in operation, the FFT analysis on voltage and current waveforms following load insertion, are illustrated in Figs. 10b-10c during voltage control and Figs. 11b-11c during var control mode. THD values, summarized in Table-3 are within acceptable limits.

Table 1 THD Summary of voltage and current in voltage regulation mode

STATCOM performance	Mode (S) of Operation	Load		%THD of load voltage ( $v_a$ )	%THD of supply current ( $i_a$ )
		MW	Pf (lag)		
Voltage Regulation	Capacitive	75	0.85	1.77	2.31
	Inductive			1.38	1.99
	Capacitive	65	0.85	1.81	2.52
	Inductive			1.41	2.12
	Capacitive	45	0.85	1.86	2.71
	Inductive			1.45	2.21

Table 2 THD Summary of voltage and current in var control mode

STATCOM performance	Load		Load pf while		%THD of load voltage ( $v_a$ )	%THD of supply current ( $i_a$ )
	MW	Pf	OFF	ON		
Unity power factor correction	75	0.85	0.85	1	1.56	3.40
	65	0.85	0.85	1	1.60	3.97
	55	0.85	0.85	1	1.65	4.77

Table 3 THD Summary of voltage and current following 10% incremental load variation

STATCOM performance	Initial Load		10% incremental load variation at the instant of 0.24s		Voltage( $v_a$ ) THD (%) after load change occurs	Current( $i_a$ ) THD (%) after load change occurs
	MW	pf (lag)	MW	pf(lag)		
Voltage regulation mode	70	0.85	7.0	0.85	1.38	2.88
var control mode (upf opn.)	70	0.85	7.0	0.85	1.56	4.71

## 6. Conclusions

A new 18-pulse, 2-level GTO-VSC based STATCOM with a rating of  $\pm 100$ MVAR, 132kV was modeled by employing three fundamental 6-pulse VSCs operated at fundamental frequency gate switching in MATLAB platform using a SimPowerSystems tool box. The inter-facing magnetics have evolved in two stages-inter-phase transformers (stage-I) and phase shifter (stage-II), and with this topology together with standard PI-controllers, harmonics distortion in the network has been greatly minimized to permissible IEEE-519 standard operating limits [9]. The compensator was employed for voltage regulation, power factor correction and also tested for dynamic load variation in the network. It was observed from the various operating performance characteristics which emerged from the simulation results that the model satisfies the network requirements both during steady state and dynamic operating conditions. The controller has provided necessary damping to settle rapidly steady states for smooth operation of the system within a couple of cycles. The proposed GTO-VSC based 18-pulse

STATCOM seems to provide an optimized model of competitive performance in multi-pulse topology.

## Appendix

System data:

- (i) 18-Pulse STATCOM parameters ( $\pm 100$ MVAR):  
Thyristors - GTO, GTO fixed resistance -  $0.01\Omega$   
Nominal AC voltage - 5.1kV,  
DC voltage - 8.3kV, DC Capacitor -  $15000\mu\text{F}$ .
- (ii) Thevenin equivalent voltage source:  
Nominal Voltage - 132kV (rms), frequency (f) - 50Hz  
Short circuit level - 3000MVA, X/R ratio-10.
- (iii) 132kV Transmission line :  
 $R=1.622\Omega$ ,  $L=10.214\text{e-}3\text{H}$
- (iv) Loads (0.85pf lag):  
70MW/75MW/65MW/55MW
- (v) Inter-phase Transformers (Stage I):  
3-phase 2-windings linear transformers -3 nos.  
Rating - 33.33MVA, 5.1/132kV,  $\Delta$ - $\Delta$  type  
Leakage Reactance (X) - 7%
- (vi) Phase shifter (Stage-II):  
Single-phase 3-windings transformers – 6 nos.  
Turn ratio (M/S) = 121/5.5kV

Turn ratio (M/L) = 121/23.3kV

Leakage reactance (X) - 6%

Rating of transformer unit - 20MVA

Phase shifting – (+) 20°, 0° and (-) 20°

(vii) Controller Gains ( $K_p$  and  $K_i$ ):

Outer voltage control loop:  $K_p=75$   $K_i=1600$

Inner current control loop:  $K_p=30$   $K_i=450$

(viii) Sampling time (Discrete time step) -  $5e^{-6}$ s

(ix) MATLAB version – 6.5

## References

- [1] Colin D. Schauder, "Advanced Static VAR Compensator Control System," U.S. Patent 5 329 221, Jul. 12, 1994.
- [2] Derek A. Paice, "Optimized 18-Pulse Type AC/DC, or DC/AC Converter System," U.S. Patent 5 124 904, Jun. 23, 1992.
- [3] Kenneth Lipman, "Harmonic Reduction for Multi-Bridge Converters," U.S. Patent 4 975 822, Dec. 4, 1990.
- [4] K.K. Sen, "Statcom - Static Synchronous Compensator: Theory, Modeling, And Applications," IEEE PES WM, 1999, Vol. 2, pp. 1177–1183.
- [5] Guk C. Cho, Gu H. Jung, Nam S. Choi, et al. "Analysis and controller design of static VAR compensator using three-level GTO inverter," IEEE Transactions Power Electronics, Vol.11, No.1, Jan 1996, pp. 57–65.
- [6] C. Schauder, M Gernhardt, E. Stacey, T. Lemak, L. Gyugyi, T.W. Cease and A. Edris, "Development of a  $\pm 100$  MVAR Static Condenser for Voltage control of transmission systems," IEEE Trans. Power Delivery, Vol. 10, No.3, July 1995, pp. 1486–1496.
- [7] Shosuke Mori, Katsuhiko Matsuno, Taizo Hasegawa, Shuichi Ohuichi, Masatoshi Takeda, Makoto Seto, Shotaro Murakami, and Fujio Ishiguro, "Development of a Large Static VAR Generator using self-commutated inverters for improving power system", IEEE Trans. Power Systems, Vol. 8, No.1, February 1993, pp. 371-377.
- [8] J.E. Hills and W.T. Norris, "Exact Analysis of a multipulse shunt converter compensator or STATCOM Part-I and II: Performance", IEE Proc. Gen. Trans. and Distribution, Vol. 144, No.2, Mar 1997, pp. 213-218 and 219-224.
- [9] IEEE Std 519-1992, IEEE Recommended Practices and Requirements for Harmonic Control in Electric Power Systems.



**Bhim Singh** was born in Rahampur, U. P., India in 1956. He received his B. E. (Electrical) degree from University of Roorkee, India in 1977 and M. Tech. and Ph. D. degrees from IIT, Delhi, in 1979 and 1983, respectively. In 1983, he joined as a Lecturer and in 1988

became a Reader in the Department of Electrical Engineering, University of Roorkee. In December 1990, he joined as an Assistant Professor, became an Associate Professor in 1994 and Professor in 1997 in the Department of Electrical Engineering, IIT Delhi. His field of interest includes power electronics and control of electrical machines. Prof. Singh is a Fellow of the Indian National Academy of Engineering, Institution of Engineers (India) and Institution of Electronics and Telecommunication Engineers, a Life Member of the Indian Society for Technical Education, System Society of India and National Institution of Quality and Reliability and Senior Member IEEE (Institute of Electrical and Electronics Engineers).



**R. Saha** received his B.E. (Hons) and M.E. in Electrical Engineering from the Jadavpur University, Kolkata, India in 1980 and 1982 respectively. He worked as Software Engineer in MMC Digital System Division, India from 1982 to 1983. He joined the

Central Electricity Authority, Govt. of India in Nov'83 through Central Power Engineering Service (Gr-A). He has been associated with Planning of the National Transmission Grid in India, Power System Studies and Grid Operation, Management & Control. He is presently pursuing research work at the Indian Institute of Technology, Delhi. His field of interest includes power system planning and development, FACTS technology and its applications. He is a Senior Member of IEEE.